

AD-A261 705



12

ANNUAL REPORT

INTERFACE ENGINEERING IN
OXIDE FIBER/OXIDE MATRIX COMPOSITES

Contract No. N0014-89-J1459

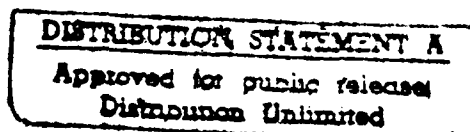
DTIC
ELECTE
MAR 8 1993
S C D

for the period
March 1, 1992 to February 28, 1993

Principal Investigator

K. K. Chawla

Department of Materials and Metallurgical Engineering
New Mexico Institute of Mining and Technology
Socorro, NM 87801



DEFENSE TECHNICAL INFORMATION CENTER



9304881

4528

Submitted to
Dr. S. G. Fishman
Project Manager
Office of Naval Research
Arlington, VA 22217

93

3 8

022

CONTENTS

Summary
List of Tables
List of Figures

I. Introduction

II. Materials

III. Experimental Procedure

- 3.1 High temperature exposure and tensile testing of Nextel 610 fiber
- 3.2 Mullite powder synthesis via diaphasic gel route
- 3.3 Fabrication of composites
- 3.4 Characterization of the fibers and composites

IV. Results and Discussion

- 4.1 Tensile strength of Nextel 610 fiber after high temperature exposure
- 4.2 Mechanical properties of interface engineered alumina fiber/glass composites
- 4.3 Interface engineering in mullite/mullite composites
 - 4.3.1 Crystallization and densification behavior of diaphasic mullite gels
 - 4.3.2 Characterization of the interface
 - 4.3.3 Thermal stress analysis
 - 4.3.4 Fracture characterization of composites
 - 4.3.5 Mechanical properties of mullite/mullite composites

V. Conclusions

VI. References

VII. Publications

VIII. Presentations

IX. Awards and Recognitions

X. Educational accomplishments

Appendix I: Report Distribution

St-A per telecon, Dr. Fishman,
ONR/1131S, Arlington, VA 22217
JK 3-8-93

Accession For	
NTIS CRA&I	<input checked="checked" type="checkbox"/>
DTIC TAB	<input type="checkbox"/>
Unannounced	<input type="checkbox"/>
Justification	
By	
Distribution /	
Availability Codes	
Dist	Avail and/or Special
A-1	

SUMMARY

We have shown in earlier work that fiber roughness is a very important parameter along with the thermal mismatch between the components. PRD-166 fiber, used so far, is a very rough fiber. Saphikon, single crystal α -alumina, is a relatively smooth fiber, but very expensive due to its processing cost. A new polycrystalline alumina fiber, Nextel 610, has recently become available. Due to its smoother surface than that of PRD-166 fiber, this fiber can be a good reinforcement candidate in oxide/oxide composites. We have done microstructural and mechanical characterization of Nextel 610 fiber. The tensile strength of Nextel 610, after exposure to 900 °C, 1100 °C, and 1300 °C was determined using a two-parameter Weibull distribution. It was observed that the primary reason for the loss of the fiber strength was the grain growth.

Two oxide fiber/oxide matrix composite systems, alumina type fiber/glass matrix and mullite type fiber/mullite matrix, were prepared. The interfaces in these composites were engineered using SnO_2 coating on alumina fibers and BN, BN/SiC coating on mullite fibers, such that deformation processes conducive to toughness enhancement could be brought to play. Significant improvements in the mechanical properties of these oxide/oxide composites could be achieved by incorporation of these interfacial coatings.

LIST OF TABLES

- Table 1. Composition and properties of the fibers and fiber coatings.
- Table 2. Properties of the matrices used.
- Table 3. Weibull distribution parameters for Nextel 610 fibers.
- Table 4. The average grain size of Nextel 610 fibers after various high temperature exposures.
- Table 5. Mechanical properties of the two oxide/oxide composites.

LIST OF FIGURES

Fig. 1 Scanning electron micrographs of Nextel 610 fiber, showing the range of the fiber diameter.

Fig. 2 Weibull plot for the as-received Nextel 610 fiber.

Fig. 3 Weibull probability density distribution of Nextel 610 fibers in as-received state and after high temperature exposures, indicating the loss of the fiber strength after high temperature exposure.

Fig. 4 Fiber surface of Nextel 610 fiber showing the grain growth after various high temperature exposures in air, (a) as-received, (b) 900 °C/2h, (c) 1100 °C/2h, and (d) 1300 °C/2h.

Fig. 5 Room temperature fractographs of Nextel 610 fiber after exposure to various temperatures. (a) As-received fiber showing the predominance of intergranular failure, (b) Exposed to 900 °C showing almost same as in (a). (c) Exposed to 1100 °C showing the transition from intergranular to transgranular failure, (d) Exposed to 1300 °C showing the predominance of transgranular failure.

Fig. 6 Fracture surface of Nextel 610 after exposure to 1100 °C, showing both intergranular and transgranular fractures.

Fig. 7 The normalized fiber strength as a function for some alumina fibers. Data represented by \circ shape were measured at room temperature after exposure to various temperatures, and by Δ shape were measured in situ at the various temperatures.

Fig. 8 SIMS analysis of the surface of a SnO_2 -coated PRD-166/glass composite, illustrating Sn^+ distribution.

Fig. 9 (a) Cross section of a BN-coated Nextel 480 fiber showing the coating thickness of 1 μm , (b) SIMS analysis of the surface of a BN-coated Nextel 480/mullite composite, showing the presence of boron.

Fig. 10(a) Cross section of a SiC/BN coated Nextel 550 fiber, showing the double coating, (b) SIMS analysis of the surface of a SiC/BN-coated Nextel 550/mullite composite, showing the presence of boron and silicon.

Fig. 11 Load-displacement curves obtained in Chevron-notch tests for Nextel 480/mullite composites in as hot-pressed and heat-treated conditions, showing the non-catastrophic failure in BN-coated Nextel 480/mullite composites.

Fig. 12 Load-displacement curves obtained in Chevron-notch tests for Nextel 550/mullite composites in as hot-pressed and heat-treated conditions, showing the non-catastrophic failure in the BN/SiC-coated Nextel 550/mullite composites.

Fig. 13 Fracture surface of PRD-166/glass composites, (a) without coating showing planar brittle failure and (b) with SnO_2 -coated showing the crack deflection and partial fiber pullout.

Fig. 14 Fracture surface of Saphikon/glass composites, (a) without coating showing planar brittle failure and (b) with SnO_2 -coated showing the neat fiber pullout.

Fig. 15 Fracture surface of BN-coated Nextel 480/mullite composites, (a) as hot-pressed state and (b) in the heat-treated state, showing the interfacial debonding and fiber pullout occurring at the interfaces between either the BN coating and fiber or the BN coating and matrix.

Fig. 16 Fracture surface of SiC/BN-coated Nextel 550/mullite composites, (a) as hot-pressed state and (b) in the heat-treated state, showing the interfacial debonding and fiber pullout occurring at the interface between the coating and matrix.

I. INTRODUCTION

Ceramic matrix composites (CMCs) capable of maintaining excellent strength and fracture toughness are required for high temperature structural applications. Many of these applications require exposure to an oxidizing environment, as such the thermodynamic stability and oxidation resistance of CMCs become important issues. Nonoxide fiber/nonoxide matrix composites, such as carbon/carbon, SiC/SiC, and SiC/Si₃N₄, have received the greatest attention. These composites generally show good low temperature strength, but oxidation resistance is a major limitation (1, 2). Nonoxide fiber/oxide matrix composites or oxide fiber/nonoxide matrix composites, for example, carbon/glass, SiC/glass, SiC/alumina, SiC/mullite, and Al₂O₃/SiC, do not have high oxidation resistance because the permeability constant for the diffusion of oxygen is high, resulting in rapid oxygen permeation through the oxide matrix (3-5). It would thus appear that in applications where stability in air at high temperature is a prime objective, oxide fiber/oxide matrix composites should be considered because they are inherently stable in air.

Some oxide/oxide matrix composite systems have been investigated (6-9). A strong fiber/matrix bond forms in the oxide matrices reinforced with uncoated oxide fibers, such as in the like/like systems (e.g., mullite/mullite) (6,7) or in the mixed systems (e.g., Al₂O₃/SiO₂) (8,9) where compound(s) forms at the interface, and the overall mechanical properties of those composites were not much improved. As a consequence, a barrier layer needs to be introduced to prevent chemical interaction between the fiber and matrix, and thus, prevent strong interfacial chemical bonding.

The alumina fiber/glass composites show good oxidation resistance. The brittle failure of such composites can be overcome by introducing interfacial coatings, such as carbon and tin dioxide coatings. As an oxide, tin dioxide is more stable than carbon on exposure to high temperatures. However, a strong and tough alumina fiber/glass composite has not been reported.

In the oxide fiber/oxide matrix composites, a mullite fiber/mullite matrix composite system is a good choice because of no risk of damage by thermal stresses during fabrication or in service owing to thermal expansion match between the fiber and matrix,

and good high-temperature properties of mullite, such as high melting point, low thermal expansion, and high creep resistance (10-14). However, very few studies on this composite system have been reported in the literature (6,7). Furthermore, both studies failed to achieve a tough composite behavior because of fiber degradation (6) or serious interfacial reaction (7), probably caused by the use of a high processing temperature ($> 1400^{\circ}\text{C}$) and/or an inefficient fiber coating (i.e., coating layer too thin to survive from the processing).

We have shown in earlier work that fiber roughness is a very important parameter along with the thermal mismatch between the components. PRD-166 fiber, used so far, is a very rough fiber. Saphikon, single crystal α -alumina, is a relatively smooth fiber, but very expensive due to its processing cost. A new ceramic fiber, polycrystalline α -alumina fiber, Nextel 610, has become available recently (15). Nextel 610 has a relatively smooth surface, and can be a reinforcement candidate in oxide/oxide composites. However, such a fine-grained fiber when used in a ceramic matrix is likely to undergo an exposure to high temperatures during processing or service. Exposure to such high temperatures can result in physical and/or chemical degradation of the reinforcements. Thus, it is important to evaluate the effect of high temperature exposure on the strength of the fibers.

In this annual report, we report the following work:

- Tensile strength of Nextel 610 fiber after high temperature exposure
- Mechanical properties of interface engineered alumina fiber/glass composites
- Interface engineering in mullite/mullite composites.

The results demonstrate the feasibility of using such interface engineering approach in the oxide fiber/oxide matrix composites.

Mechanical bonding is very desirable for high toughness in ceramic matrix composites. In a mechanical bond, the degree of interfacial roughness is a very important parameter, which, in turn, is controlled by the fiber surface roughness. The surface roughness of three alumina-type fibers, PRD-166, Nextel 610, and Saphikon fiber are quantitatively being characterized using an atomic force microscope. This work is under progress and the results will be included in the next year's report.

II. MATERIALS

Two kinds of alumina fibers, PRD-166 (α -alumina + 15 w/o zirconia) and Saphikon (single crystal α -alumina), were used in a borosilicate glass, N51A, matrix composites. Nextel 480 and Nextel 550 fibers were used in mullite matrix composites. Nextel 480 is a polycrystalline fiber with an essentially mullite composition. The as-received Nextel 550 is not crystalline mullite but a mixture of δ -alumina and amorphous silica with mullite composition, which can be transformed to mullite when heated above 1200 °C. Mullite powder synthesized via a diphasic gel route in our laboratory was used as matrix materials. The fiber coatings, SnO_2 for PRD-166 and Saphikon fibers, were applied by chemical vapor deposition (CVD) in our laboratory, while BN and BN/SiC for Nextel 480 and Nextel 550 were applied via CVD by 3M Co., respectively. In the double coating, the outer layer was SiC. Nextel 610, a relatively smooth fiber, is the new fiber to be used in this work. The nominal compositions and some properties of the materials used are summarized in Tables 1 and 2.

III. EXPERIMENTAL PROCEDURE

3.1 High temperature exposure and tensile testing of Nextel 610 fiber

High temperature exposures of Nextel610 fiber samples were made for 2 hours at 900 °C, 1100 °C, and 1300 °C, respectively. The exposure temperature were reached within 45 min; and after 2 h soaking at the given temperature, the fibers were cooled to the room temperature in 2 h. All these experiments were performed in an alumina tube and in the air.

The tensile strength was measured followed ASTM standard, D3379-75. The tensile tests were performed at room temperature on an Instron universal machine (model 1122) using a crosshead speed of 0.5 mm/min. The specimen gage length was 40 mm. A load cell of 5 N capacity was calibrated by a precision standard weight and recalibrated after testing every batch of thirty fibers. This was done to eliminate any possible shift in calibration. All fibers used in this investigation were taken from the same batch.

3.2 Mullite powder synthesis via diaphasic gel route

In order to eliminate the high temperature processing induced damage to fibers, the fabrication temperature of mullite/mullite composites should be as low as possible. A highly sinterable mullite powder as the matrix was prepared from a diaphasic gel route in our laboratory. In the present study, six different kinds of diaphasic mullite gels were prepared using various sources of boehmite (ALOOH) powder and silica sol, and their crystallization and densification behavior were compared to find the optimum precursor combination giving the lowest fabrication temperature and the highest densification.

3.3 Fabrication of composites

All the composites with coated and uncoated fibers were fabricated by slurry impregnation method (16). Consolidation of composites was done by hot-pressing. The details of the fabrication can be found elsewhere (17).

3.4 Characterization of the fibers and composites

Optical and scanning electron microscopes were used for general characterization of the microstructure of Nextel 610 fibers and the composites. Secondary ion mass spectrometry (SIMS) was used to characterize the coatings in composites. Bend strength of composites was measured in three-point bend tests at room temperature using rectangular bar-shaped specimens with fiber direction parallel to the length of the specimen. The work of fracture (WOF) and the critical stress intensity factor of the composites were measured at room temperature using Chevron-notched bar specimen in three-point bend tests.

IV. RESULTS AND DISCUSSION

4.1 Tensile strength of Nextel 610 fiber after high temperature exposures

Scanning electron micrographs of as-received Nextel 610 fibers are shown in Fig. 1, from which the variation of the fiber diameter can be seen. The average diameter of the fiber was $11.22\text{ }\mu\text{m}$ with a standard deviation of $0.98\text{ }\mu\text{m}$. A plot of Weibull equation for the as-received fiber is shown in Fig. 2. The Weibull modulus, α , for the fiber was 6.58.

There occurred a substantial fall in the Weibull mean strength above $900\text{ }^{\circ}\text{C}$ exposure, see Fig. 3 and Table 3. Microstructural examination of fibers exposed to high temperatures, see Fig. 4, revealed the changes which led to the loss of room temperature. It can be seen from Fig. 4 that the primary change of the microstructure was the grain growth, especially, above $1100\text{ }^{\circ}\text{C}$. Table 4 lists the average grain size of the fiber after different temperature exposures. It is expected that the strength of fine-grained fiber would be higher than that of a coarse-grained fiber because length of Griffith microcracks is limited by the grain diameter.

The Weibull modulus, α , an empirical constant, is related to the properties of the flaw size distribution of a material [18]. For materials with small values of α , a large defect is likely to be present. The decrease of the value of Weibull modulus, which is greater than the error range which is given in the last column in Table 3, implies that any defects created during high temperature exposure are more severe than any preexisting flaws in the fiber. This can be another reason to cause the fiber strength reduction after high temperature exposure.

The fracture surfaces of fibers exposed to different temperatures, shown in Fig. 5, revealed different failure mechanisms. Intergranular failure was dominated in the as-received fibers, see Fig. 5(a), while transgranular failure occurred in the fiber after exposure to $1300\text{ }^{\circ}\text{C}$, see Fig. 5(d). The transition from intergranular failure to transgranular failure occurred at about $1100\text{ }^{\circ}\text{C}$, as shown in Fig. 6, where both of failure mechanisms can be seen. The variation in the percentage of transgranular fracture with grain size is not well known [19-21]. Fractography observations, as

shown in Figs. 5 and 6, together with fiber strength and grain determinations, indicated that the grain size range over which the fracture mode changed from transgranular to intergranular, was also where the strength showed a strong grain size dependence.

It is interesting to note that a strength loss above 900 °C is very common in alumina fiber [22-24]. Figure 7 shows the normalized strength data of some alumina fibers versus the exposure temperature. The strength of the alumina fibers measured at elevated temperatures, shown in Fig. 7, revealed the same tendency as that measured at room temperature. Clearly, such a loss of strength after high temperature exposure is a limitation of the polycrystalline alumina fiber as a reinforcement for high temperature composites.

4.2 Characterization of the interface

A detailed metallographic investigation of the tin dioxide interphase produced at different temperatures and different times was made (24). Results of the SIMS characterization of the PRD-166 fiber/SnO₂/glass composite, shown in Fig. 8, indicated that the Sn⁺ in the coating was localized to the coating only and no diffusion into fiber or matrix was apparent. This is expected since our earlier electron microprobe work showed that SnO₂ can act as diffusion barrier layer in this system in the form a laminate (25). The present SIMS work, however, confirmed in the case of a fiber composite system.

Figure 9(a) shows a cross section of the BN coated Nextel 480 fiber, with coating thickness being about 1 μm. SIMS characterization verified that the layers on the periphery of the fibers were the BN coatings, see Fig. 9(b). The microstructure of the BN/SiC coated Nextel 550 fiber, Fig. 10(a), shows that the fiber was fairly uniformly coated with two layers, BN and SiC, with thickness of about 0.1 μm and 0.2 μm, respectively. SIMS characterization also illustrated the presence of the double coating in the composites, as shown in Fig. 10(b,c). Thicker BN coating was used to survive the processing conditions in order to provide a desired weak interface. By the same token, the double coating was used to protect the BN inner layer from oxidation during composite fabrication with the SiC outer layer, which is well known to have excellent resistance to high temperature oxidation owing to the formation of a protective film of

silica on the surface.

4.3 Thermal stress analysis

Thermal stresses are generated in composite materials because of thermal expansion coefficient mismatch between the matrix and reinforcement, the importance of which is well recognized. The thermal stresses in coated and uncoated PRD-166/glass as well as Saphikon/glass were evaluated using two- and three-element models (26). The results showed a radial tensile stress component at fiber/coating and coating matrix interfaces. This is desirable in order to weaken the interfacial bonding. In the like/like system, such as mullite/mullite composite, the thermal expansion coefficient match between the composite components can eliminate the risk of the possible damage caused by thermal stresses. Thermal stress induced by BN coating were analyzed (27). It turned out that a tensile radial stress less than 10 MPa existed at the fiber/coating interface, which was also favorable for the weak interface.

4.4 Mechanical properties

The three-point bend strength, work of fracture, and critical stress intensity factors determined for PRD-166/glass and mullite/mullite composites are listed in Table 5. As can be seen, significant improvements, specially in fracture toughness, were attained with the interface engineered alumina/glass and mullite/mullite composites. Toughness values between 6 and 11.6 MPa.m^{1/2} were obtained in mullite/mullite composites.

The composites with 1 μ m BN-coated Nextel 480 exhibited damage tolerant characteristics with a load-bearing capacity even beyond the maximum load, as indicated by a gradual load drop which continued up to a significant amount of displacement without complete failure during the test, as seen in Fig. 11. After heat treatment leading to complete mullite crystallization of the matrix, this composite still showed non-catastrophic failure, also shown in Fig. 11. The loss of fiber strength resulted from the heat treatment was responsible for the load drop to a certain level after heat treatment. Similar to the case of Nextel 480/BN/mullite composites, the composites of Nextel 550/BN/SiC/mullite showed a non-brittle failure, see Fig. 12.

4.5 Fracture characteristics of composites

4.5.1 Alumina/glass system

Scanning micrographs of the fracture surfaces obtained in three-point bend test of the various composites with coated and uncoated fibers, are shown in Figs. 13 and 14. In the case of PRD-166/glass and Saphikon/glass composites, the bonding between the uncoated fiber and the matrix is very strong, resulting in a brittle, flat fracture. Introduction of the SnO_2 fiber coating results in a weakening of the fiber/matrix interface. As a result the fracture observed in the case of the coated fiber composites exhibited a relatively non-planar fracture, see Fig. 13(b). The lack of extensive fiber pull out in PRD-166/ SnO_2 /glass was attributed to the radial clamping due to the surface roughness of the PRD-166 fiber (26,28). Comparison of the effects of interfacial roughness and thermal stress on the radial stress at the interface showed that the effect of roughness induced radial compressive strain was an order greater than the thermal strain in this system (26). Therefore, the surface texture of the fiber can have a pronounced effect on the debonding and pullout characteristics of the composites. This was demonstrated by incorporating relatively smooth single alumina fibers (Saphikon) into the same glass matrix. Bend tests carried out on this composite exhibited extensive fiber/matrix debonding and fiber pullout, see Fig. 14(b). The important point to note here is that pullout occurred at the fiber/coating interface. This is expected because SnO_2 and alumina has no natural solid solubility.

4.5.2 Mullite/mullite system

Scanning electron micrographs of the fracture surfaces obtained in three-point bend test of mullite/mullite composites are shown in Figs. 15 and 16. The coating in Nextel 480/mullite was found on the pulled-out fiber surface with some peeling-off or separation from the fiber, see Fig. 15. The pulled-out fiber surface in Nextel 550/mullite composites was mostly clean and smooth, see Fig. 16. This indicates that, unlike Nextel 480/mullite composites in which the fiber pullout could occur at the interface of either matrix/coating or coating/fiber, the fiber pullout occurred along the the fiber/coating interface only.

V. CONCLUSIONS

The alumina fiber, Nextel 610, suffered strength loss from exposure to high temperature. The primary reason for the strength loss of Nextel 610 fiber was grain growth. Defects, such as surface flaws induced during high temperature exposure procedure, can be another source for the loss of the fiber strength. Fractography observations together with fiber strength and grain size determination indicated that the grain size range over which the fracture mode changed from transgranular to intergranular was also where the strength showed a grain size dependent.

The fiber/matrix interaction in oxide/oxide composites can be effectively controlled by interface engineering approach. Tin dioxide, BN, and BN/SiC would appear to be effective coating materials for the oxide/oxide composite systems investigated in this work. Incorporation of fiber coatings such as SnO_2 coating, BN coating, and SiC/BN double coating, together with other considerations, such as thermal stress, surface roughness of the fiber, and composite processing parameters, allows to make the oxide/oxide composites with tough behavior.

VI. REFERENCES

1. K.L. Luthra, Carbon, **26** (1988) 217-24.
2. T. Mah, N.L. Hecht, D.E. McCullum, J.R. Hoenigman, H.M. Kim, A.P. Katz, and H.A. Lipsitt, J. Mater. Sci., **19** (1984) 1191-1201.
3. K.M. Prewo and J.A. Batt, J. Mater. Sci., **24** (1988) 523-27.
4. E.E. Hermes and R.J. Kerans, Mater. Res. Soc. Symposium Proceedings, **125** (1989) 73-78.
5. K. Vedula, "Ultra High-Temperature Ceramic-Ceramic Composites," WRDC-TR- 89-4089(1989).
6. R.N. Singh and M.K. Brun, Ceram. Sci. Eng. Proc., **8** (1987) 636-43.
7. O. Yeheskel, M.L. Balmer, and D.C. Cranmer, Ceram. Sci. Eng. Proc., **9** (1988) 687-94.
8. E. Fitzner and J. Schlichting, High Temperature Sci., **13** (1980) 249-72.
9. T.A. Michalske and J.R. Hellmann, J. Am. Ceram. Soc., **71** (1988) 725-31.
10. K.S. Mazdiasni and L.M. Brown, J. Am. Ceram. Soc., **55** (1972) 548-52.
11. P.A. Lessing, R.S. Gordon, and K.S. Mazdiasni, J. Am. Ceram. Soc., **58**(1975)149.
12. P.C. Dokko, J.A. Pask, and K.S. Mazdiasni, J. Am. Ceram. Soc., **60** (1977) 150-55.
13. T. -I. Mah and K. S. Mazdiasni, J. Am. Ceram. Soc., **66** (1983) 699-703.
14. R. Ruh, K. S. Mazdiasni, J. Am. Ceram. Soc, **71** (1988) 503-12.
15. D. M. Wilson, in **Proc.: 14th Conf. on Metal Matrix, Carbon, and Ceramic Matrix Composites**, Cocoa Beach, FL, Jan 17-19, 1990, NASA Conference Publication 3097 Part 1, pp.105-17.
16. K.K. Chawla, **Composite Materials**, Springer-Verlag, New York, 1987, p.134.
17. R.V. Vaidya, J. Fernando, and K.K. Chawla, Mater. Sci. and Eng., **A150** (1992) 161-69.
18. A.De S. Jayatilaka and Trustrum, J. Mater. Sci., **12** (1977) 1426-30.
19. R.M. Spriggs, J.M. Mitchell, and T. Vasilos, J. Am. Ceram. Soc., **47** (1964) 323-27.
20. P.L. Gutshall and G.E. Gross, Eng. Fracture Mechanics, **1** (1969) 463-71.

21. B. J. Dalgleish, S. M. Johnson, and A. G. Evans, *J. Am. Ceram. Soc.*, **67** (1984) 741-50.
22. J.C. Romine, *Ceram. Eng. Sci. Proc.*, **8** (1987) 755-65.
23. D.J. Pysher, K.C. Goretti, R.S. Hodder, Jr., and R.E. Tressler, *J. Am. Ceram. Soc.*, **72** (1989) 284-88.
24. K. Jakus and V. Tulluri, *Ceram. Eng. Sci. Proc.*, **10** (1989) 1338-49.
25. A. Maheshwari, K. K. Chawla, and T. A. Michalske, *Mater. Sci. Eng.*, **A107** (1989) 269-76.
26. K.K. Chawla, M.K. Ferber, Z.R. Xu, and R. Venkatesh, "Interface Engineering in Alumina/Glass Composites," *Mater. Sci. & Eng.*, 1993, in press.
27. J. Fernando, K.K. Chawla, M.K. Ferber, and D. Coffey, *Mater. Sci. & Eng.*, **A154** (1992) 103-108.
28. R. Venkatesh and K.K. Chawla, *J. Mater. Sci. Letter*, **11** (1992) 650-652.

VII. PUBLICATIONS

Journals

1. R. Venkatesh, K.K. Chawla, and M. Ferber, "Some Observations on the Paper "Influence on Tin Dioxide Interphase on the Residual Stresses in Aluminum Fiber/Glass Composites," **Scripta Met & Mater.** **26** (1992) 859.
2. R.U. Vaidya, J.A. Fernando, K.K. Chawla, and M.K. Ferber "Effect of Fiber Coating on the Mechanical Properties of a Nextel 480 Fiber Reinforced Glass Matrix Composite," **Mater. Sci. & Eng.** **A150** (1992) 161.
3. R. Venkatesh and K.K. Chawla, "Effect of Interfacial Roughness on Fiber Pullout in Alumina/Glass Composites," **J. Mater. Sci. Lett.**, **11** (1992) 650.
4. J.A. Fernando, K.K. Chawla, M.K. Ferber, and D. Coffey, "Effect of Boron Nitride Coating on Tensile Strength of Nextel 480 Fiber," **Mater. Sci. & Eng.**, **A154** (1992) 103.
5. J.-S. Ha and K.K. Chawla, "Effect of SiC/BN Double Coating on Fibre Pullout in Mullite Fibre/Mullite Matrix Composites," **J. Mater. Sci. Lett.**, **12** (1993) 84.
6. M.K. Ferber, A.A. Wereszczak, L. Riester, R.A. Lowden, and K.K. Chawla, "Evaluation of the Interfacial Mechanical Properties in Fiber Reinforced Ceramic Composites," **Ceramic Sci. & Eng. Proc.**, Amer. Ceram. Soc., Westerville, Ohio, 1993.
7. K.K. Chawla, M.K. Ferber, and R. Venkatesh, "Effect of Interfacial Roughness and Thermal Stress in Alumina/Glass and Alumina/Tin Dioxide/Glass Composites," **Mater. Sci. & Eng.**, **A150**, in press.

8. J.-S. Ha, K.K. Chawla, and R.E. Engdahl, **Ceramics International**, in press.
9. J.-S. Ha and K.K. Chawla, **Mater. Sci. & Eng.**, in press.
10. K.K. Chawla, Z.R. Xu, R. Venkatesh, and J.S.-Ha, in **Proc.: 9th Inter. Conf. on Composite Materials**, Madrid, Spain, to be published.

BOOKS

1. K.K. Chawla, **Ceramic Matrix Composites**, Chapman & Hall, London, in press.

VIII. PRESENTATIONS

1. A. Wolfenden, K.K. Chawla et al., "Measurements of Dynamic Elastic Moduli, Mechanical Damping, and Mass Density in Some Glass Matrix Composites," Symposium on Ceramics and Advanced Materials, Oct. 23, 1992, Santa Fe.
2. K.K. Chawla, "Interface Engineering in Alumina/Glass Composites," Eshbach Lecture at Northwestern University, Oct. 27, 1992, Evanston, IL.
3. K.K. Chawla, "The Role of Matrix in Metal Matrix Composites," Eshbach Lecture at Northwestern University, Sept. 25, 1992, Evanston, IL.
4. K.K. Chawla, "The Role of Matrix in Metal Matrix Composites," Department of Materials Science and Engineering, Oct. 14, 1992, Wayne State University, Detroit, MI.
5. K.K. Chawla, "Composite Materials: A Bird's Eye-View," Invited Seminar, Oct. 19, 1992, Argonne National Laboratory, Argonne, IL.
6. K.K. Chawla, "Interface Engineering in Alumina/Glass," Department of Materials Science and Engineering, University of Illinois at Urbana-Champaign, Invited Seminar, Nov. 30, 1992, Urbana, IL.

IX. AWARDS & RECOGNITIONS

1. Member, Advisory Committee for the Composites Conference, Society of Manufacturing Engineers.
2. Member, International Committee on Composites Materials (ICCM).
3. Selected ASM International and Indian Institute of Metals Lecturer for 1990-91. Visited universities and research institutions in India and gave lectures on composite materials.
4. Invited to deliver the Tutorial Luncheon Talk on "Composite Materials in Aerospace," at the TMS annual technical meeting and materials week at Cincinnati, Oct., 1992.
5. Invited to give the keynote lecture "Ceramic/Metal interfaces in Composites," at the Symposium, Structure and Properties of Metal-Ceramic Interfaces, TMS Fall '91 meeting, Oct. 20-24, 1991, Cincinnati, Ohio.
6. Eschbach Visiting Scholar, Northwestern University, Evanston, IL., Fall 1992.

X. Educational accomplishments

One of the important objectives of any research in the universities should be to train students to do high quality research. Research activity can and should be rightly considered an educational activity. Planning experiments, collecting and analyzing data, and finally presenting the results, oral and written, to the community at large form part of this activity. Students attend weekly meeting where they present, defend, and get feedback on their work. They are in daily contact with the P. I. to discuss their work and related problems.

The personnel included in this research are listed below.

Postdoctoral Research Associate

1. R. U. Vaidya
2. Z. R. Xu

Graduate Students

1. R. Venkatesh (Ph.D.)
2. J. S. Ha (Ph.D.)
3. J. Groves (M.S.)

Undergraduate Students

1. J. Ambriz
2. P. Tenorio
3. G. Martinez
4. B. Furman

APPENDIX I: REPORT DISTRIBUTION

Addressees	Number of Copies
Scientific Officer Code : 1131N Steven G. Fishman Office of Naval Research 800 North Quincy Street Arlington, Virginia 22217-5000	3
Administrative Grants Officer Office of Naval Research Resident Representative N68583 Administrative Contracting Officer University of New Mexico, RM 204 Bandelier Hall West Albuquerque, New Mexico 87131-0001	1
Director, Naval Research Laboratory Attn : Code 2627 Washington, DC 20375	6
Defense Technical Information Center Building 5, Cameron Station Alexandria, Virginia 22314	12
Mr. W.D. Peterson New Mexico Tech Socorro, New Mexico 87801	1

Table 1. Composition and properties of fibers and fiber coatings

	PRD-166	Saphikon	Nextel 480	Nextel 550	Nextel 610	SnO ₂	BN	SiC
Composition (wt%)	ZrO ₂ : 15-20 Al ₂ O ₃ : 80-85	α -Al ₂ O ₃	Al ₂ O ₃ : 70 SiO ₂ : 28 B ₂ O ₃ : 2	Al ₂ O ₃ : 73 SiO ₂ : 27	α -Al ₂ O ₃	-	-	-
Melting point (°C)	1830	2053	1850	1850	2053	1630	3000	2220
Density (g/cm ³)	4.2	3.9	3.05	3.03	3.75	6.95	2.27	3.21
Tensile strength (MPa)	2070 (6.4) [†]	3150	1900 (51) [†]	2000 (51) [†]	1900	-	80-110	255-465 [#]
Young's modulus (GPa)	380	380	220	193	373	233	60-80 [#]	440-470 [#]
CTE (10 ⁻⁶ /°C)	9	9.12 (parallel to c-axis) 7.95 (perpendicular to c-axis)	4-5	4-5	9	5.23	5 [#]	4.8 [#]

[#] Data of CVD materials

[†] Gauge length

Table 2. Properties of matrices

	Melting point (°C)	Density (g/cm ³)	Tensile strength (MPa)	Young's modulus (GPa)	CTE (10 ⁻⁶ /°C)
N51A glass	—	2.2	64	72	7
Mullite	1850	3.17	128–185	181	4–5

Table 3. Weibull distribution parameters for Nextel 610 fibers

Fiber	No. of samples	Weibull modulus α	β , GPa	Mean strength σ , GPa	Standard deviation S, GPa	r	Standard deviation of α
As-received	57	6.58	1.771	1.651	0.297	96	0.87
Exposed at 900°C for 2 h	60	4.85	1.398	1.281	0.302	97	0.63
Exposed at 1100°C for 2 h	57	4.78	1.038	0.951	0.227	94	0.63
Exposed at 1300°C for 2 h	58	4.79	0.663	0.607	0.145	97	0.63

r: correlation coefficient of linear regression.

Table 4. The average grain size of Nextel 610 fiber
after various high temperature exposures

	As-received	Exposure temperature		
		900 °C	1100 °C	1300 °C
Grain size, μm	0.080	0.089	0.096	0.175

Table 5. Mechanical properties of the composites

Composites		V_f	σ_{\max} (MPa)	WOF (J/m^2)	K_{Ic} ($\text{MPa m}^{1/2}$)
PRD-166/glass					
Uncoated		0.40	225	750	2.5
SnO ₂ -Coated		0.35	150	920	3.3
Nextel 480/mullite					
Uncoated	As-HP	0.45	104	56	1.8
	HT	0.45	106	47	1.9
BN-coated	As-HP	0.41	322	2410	11.6
	HT	0.41	258	1630	8.5
Nextel 550/mullite					
Uncoated	As-HP	0.47	87	18	1.5
	HT	0.47	71	12	1.4
SiC/BN-coated	As-HP	0.33	182	733	7.1
	HT	0.33	223	308	6.0

As-HP : as hot pressed; HT : after heat treatment.

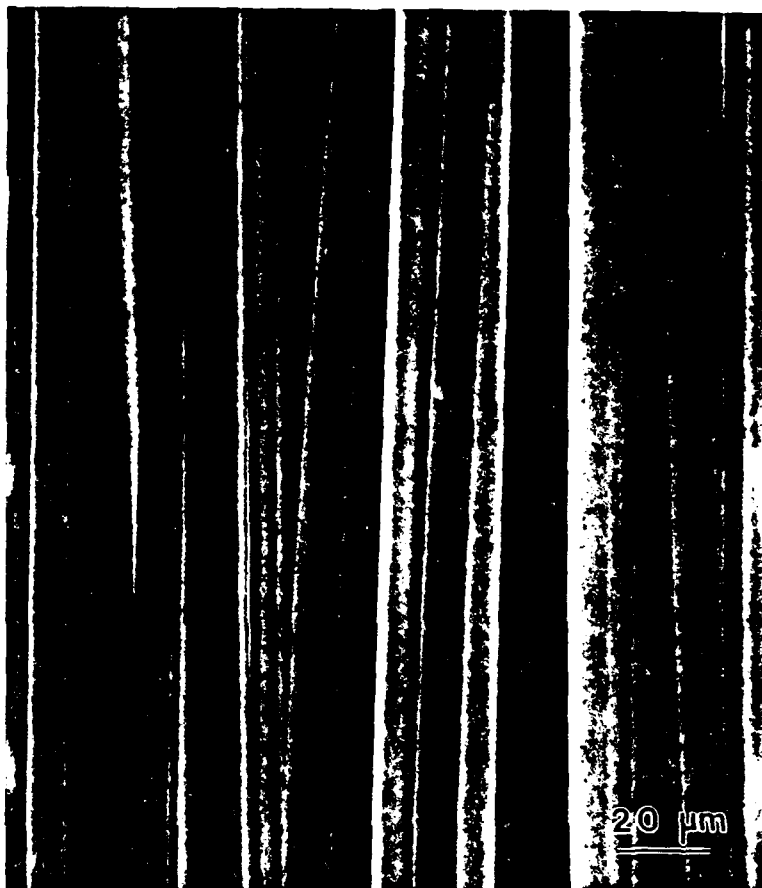


Figure 1

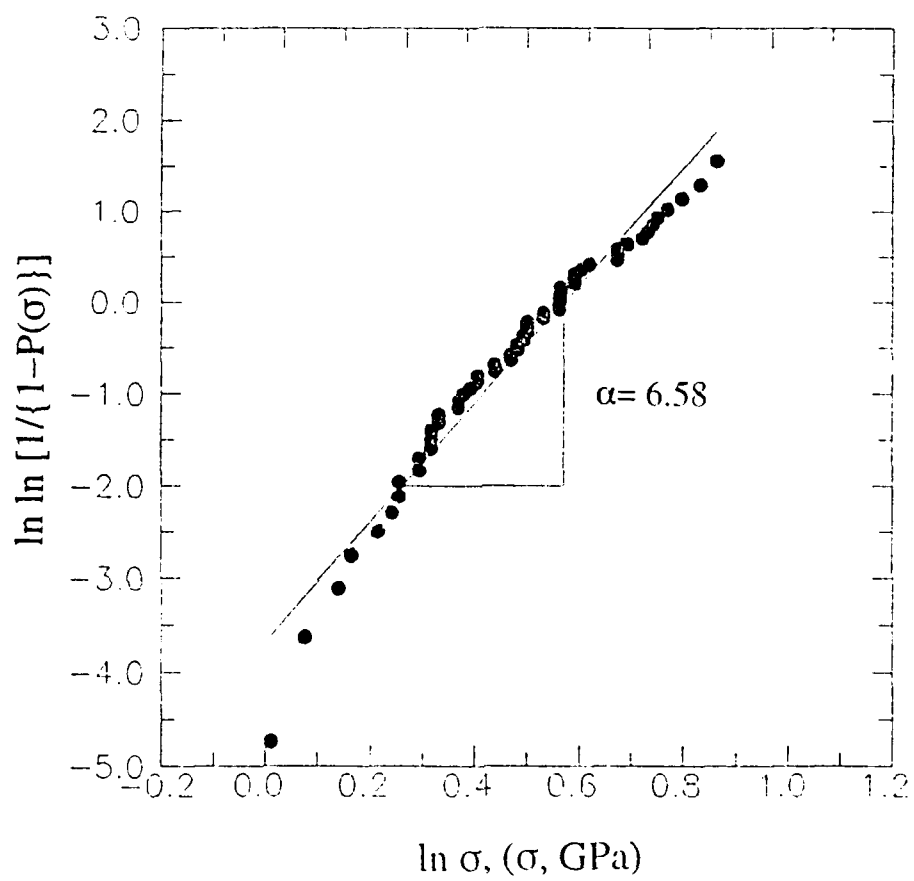


Figure 2

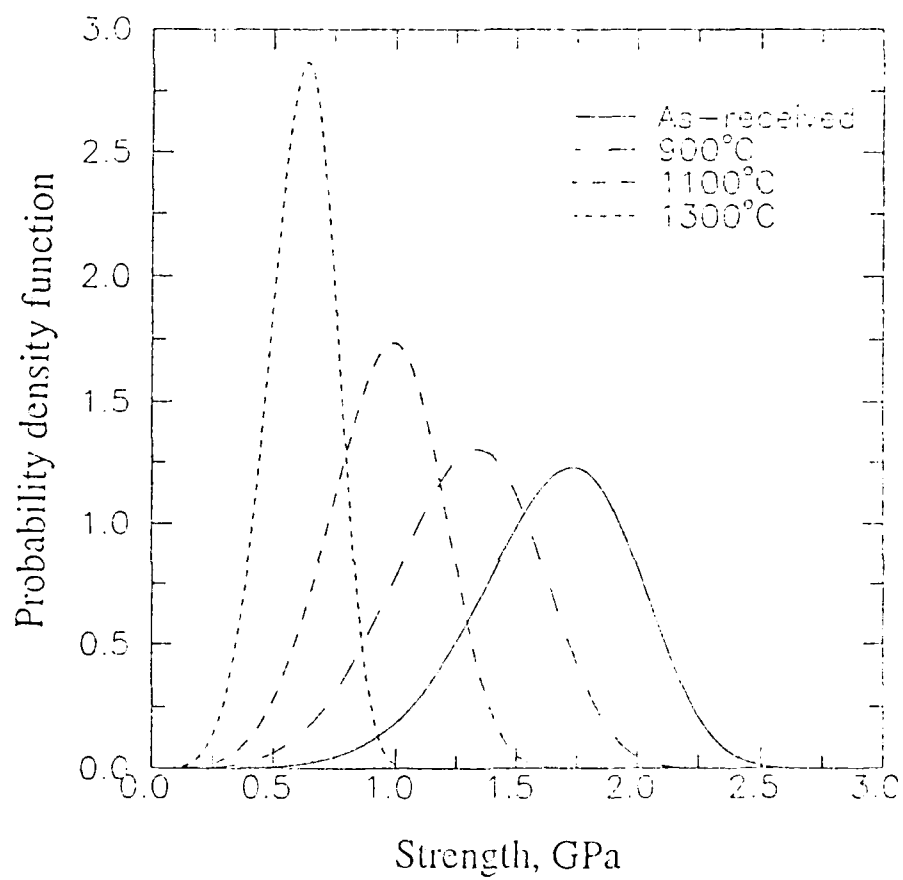


Figure 3

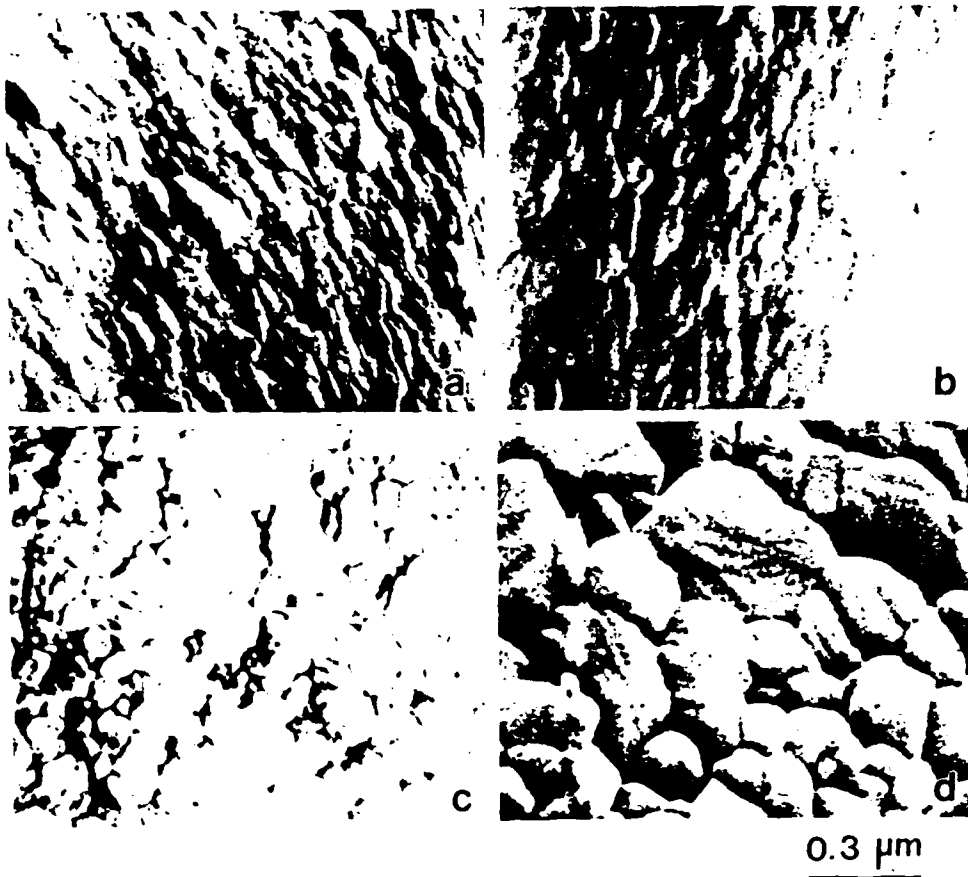


Figure 4

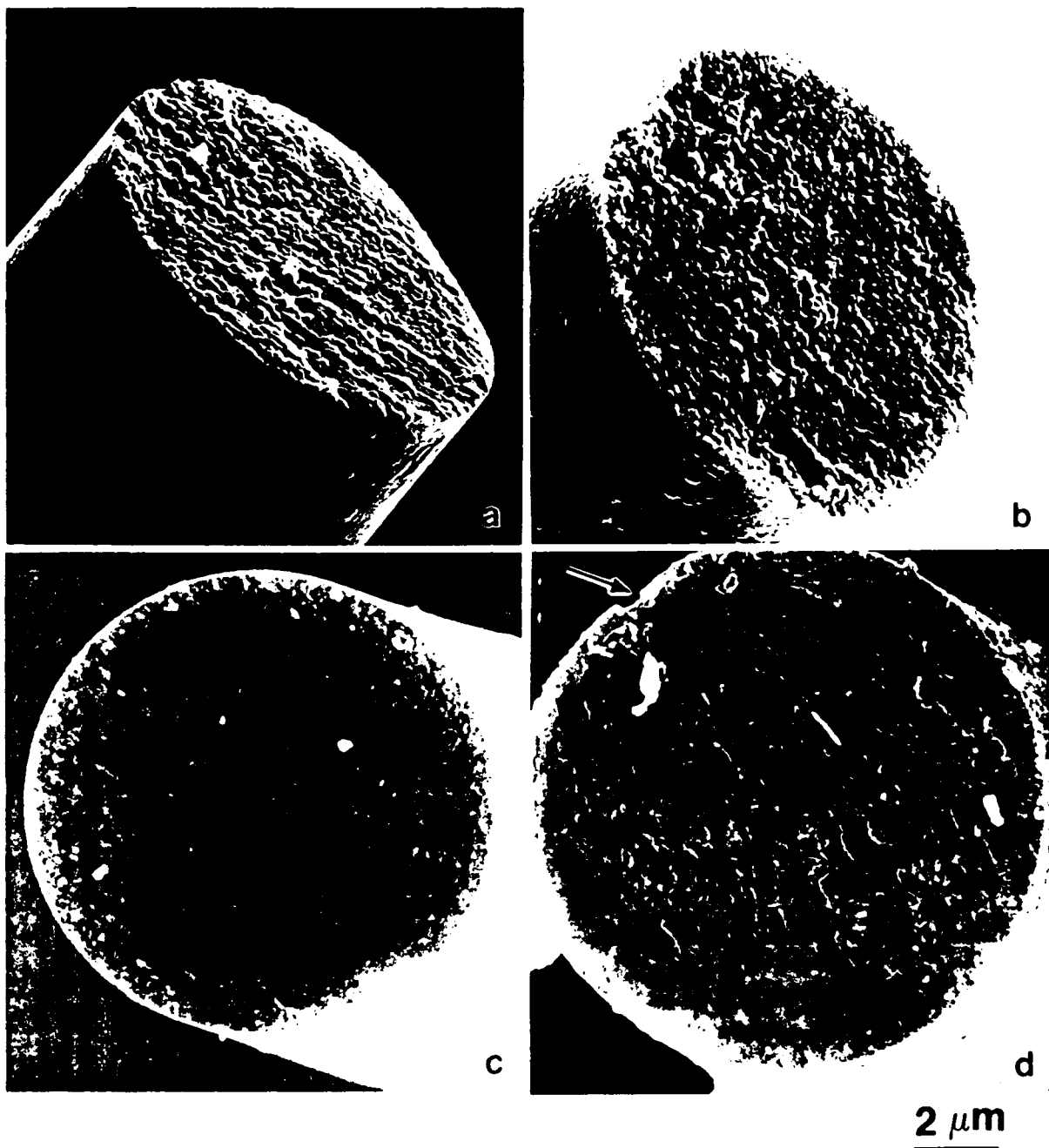


Figure 5

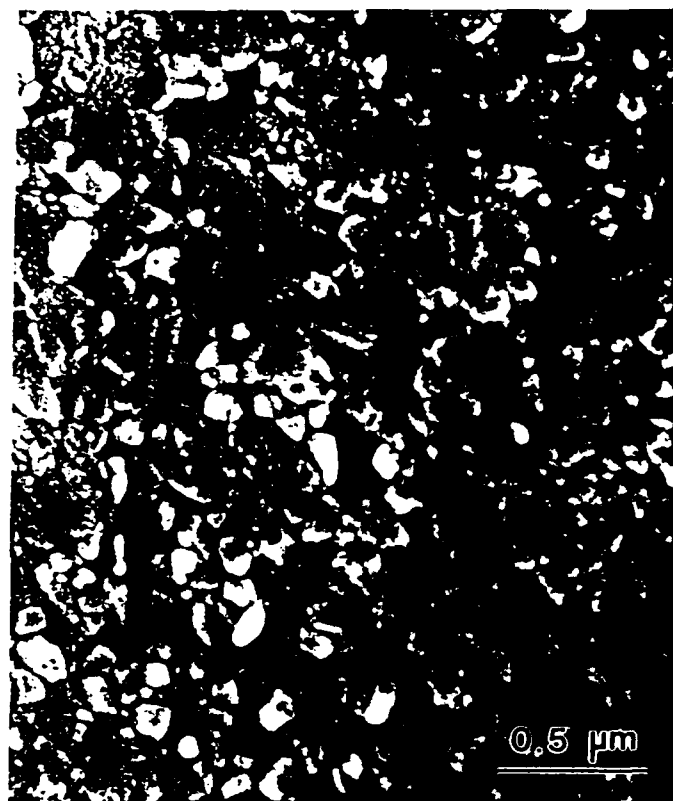


Figure 6

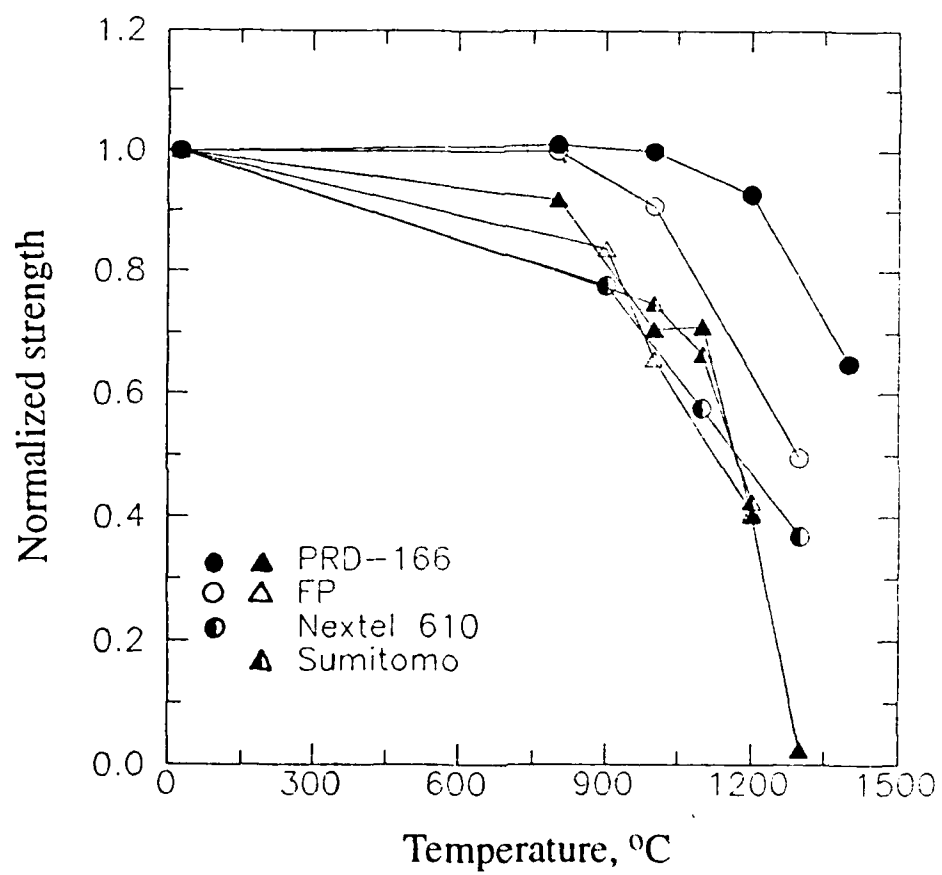


Figure 7

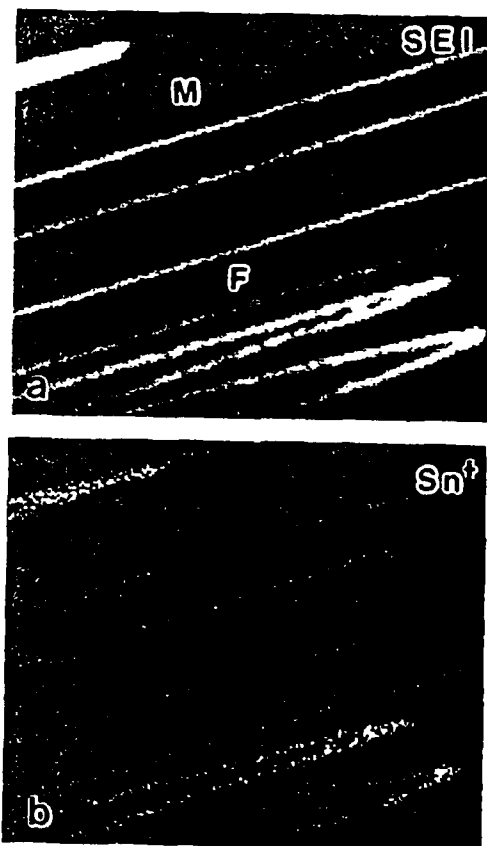


Figure 8

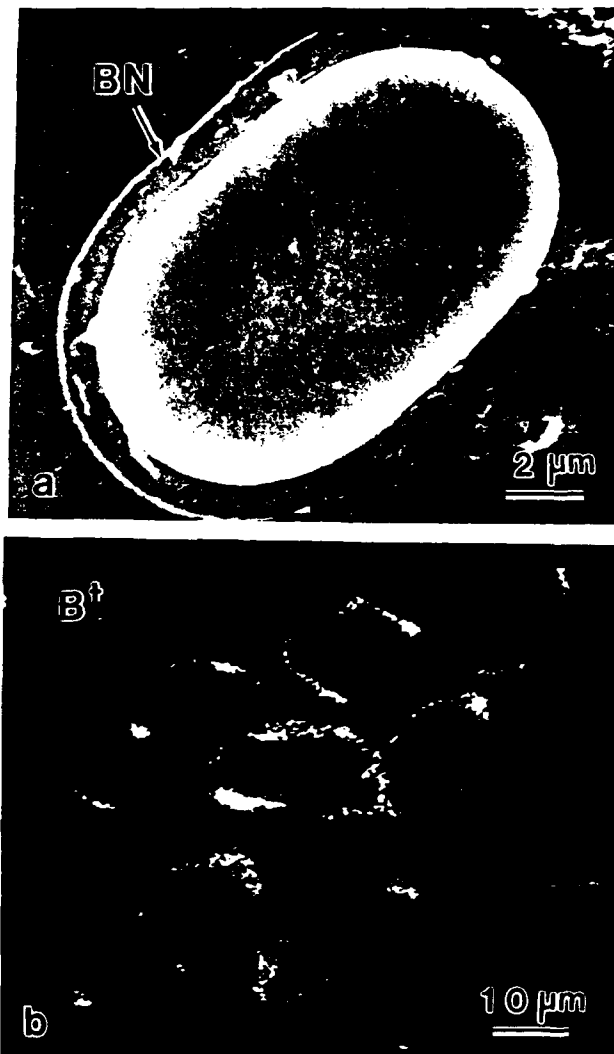


Figure 9

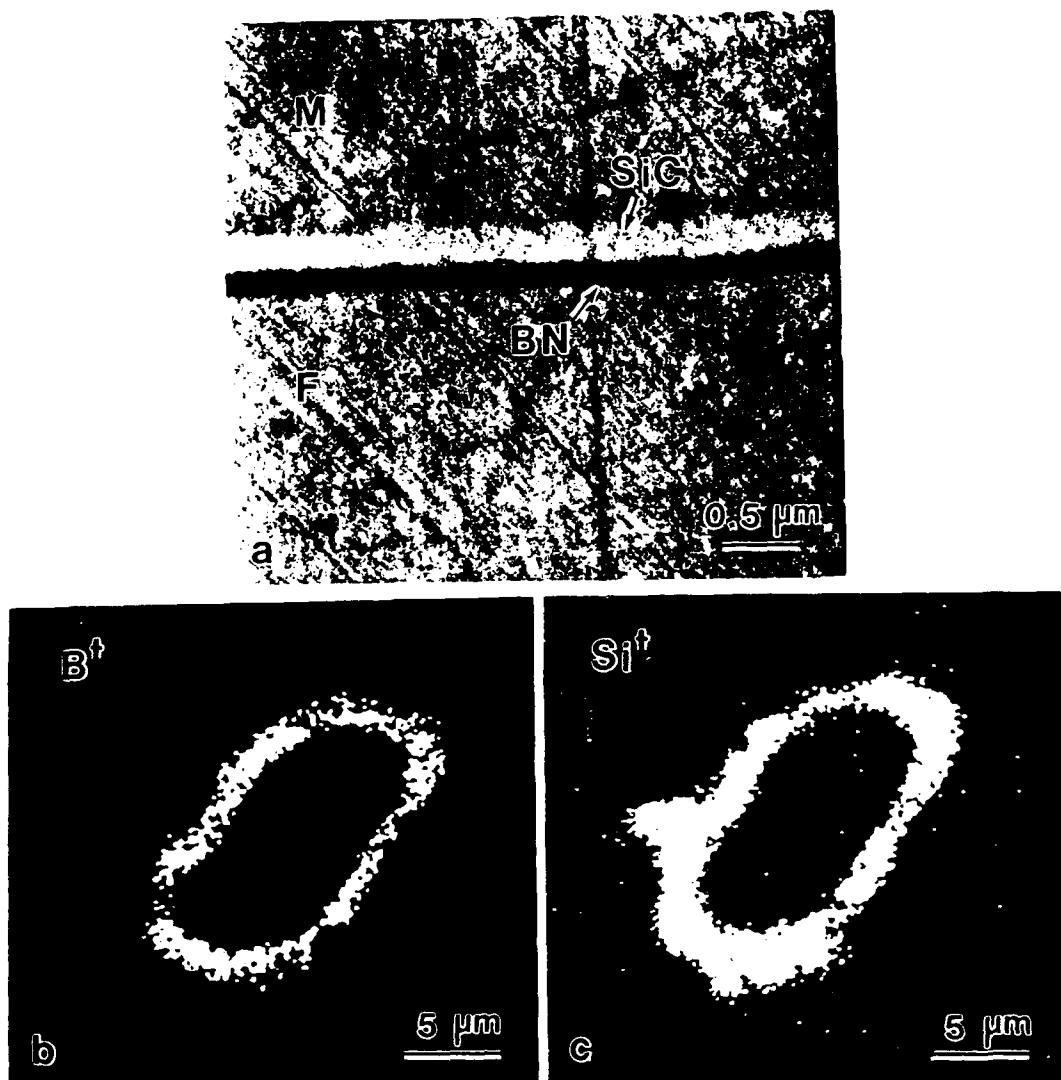


Figure 10

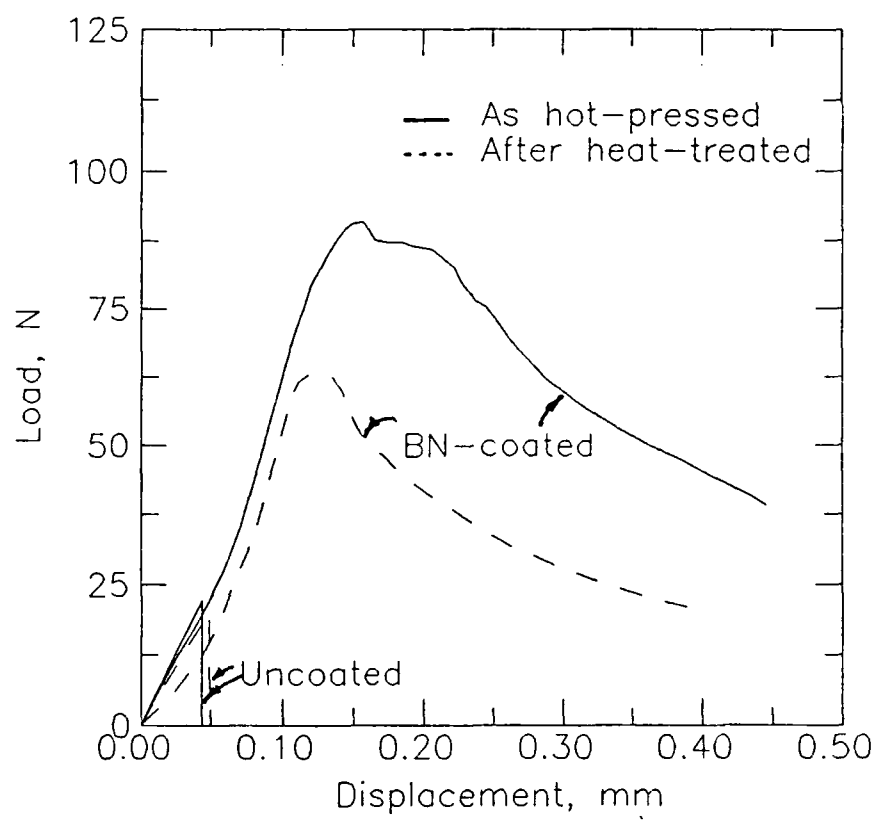


Figure 11

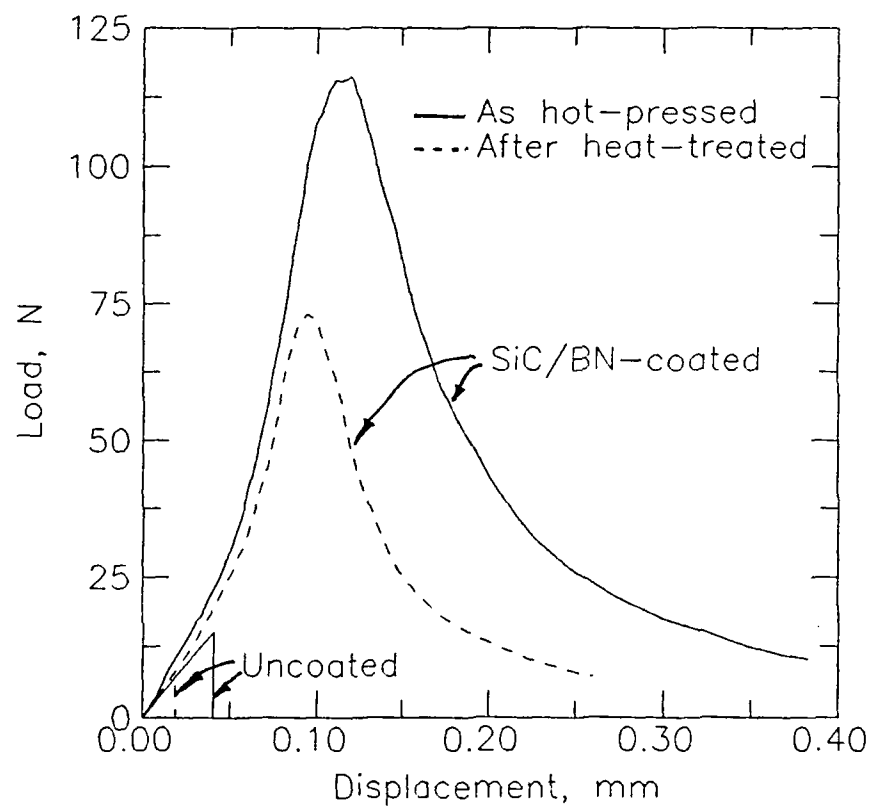


Figure 12

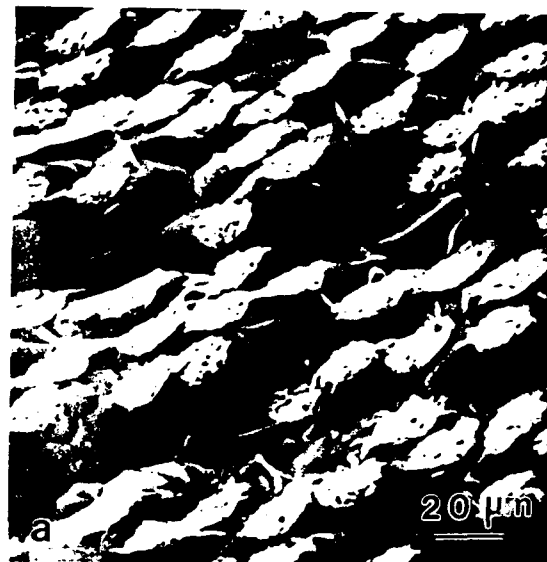


Figure 13



Figure 14

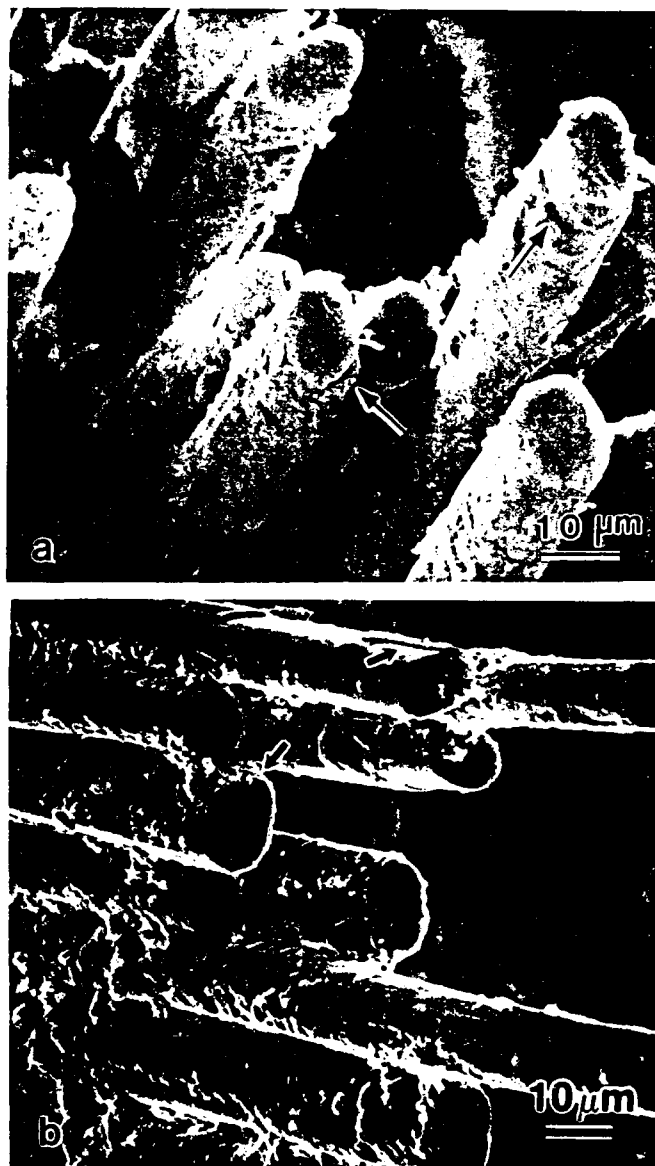


Figure 15

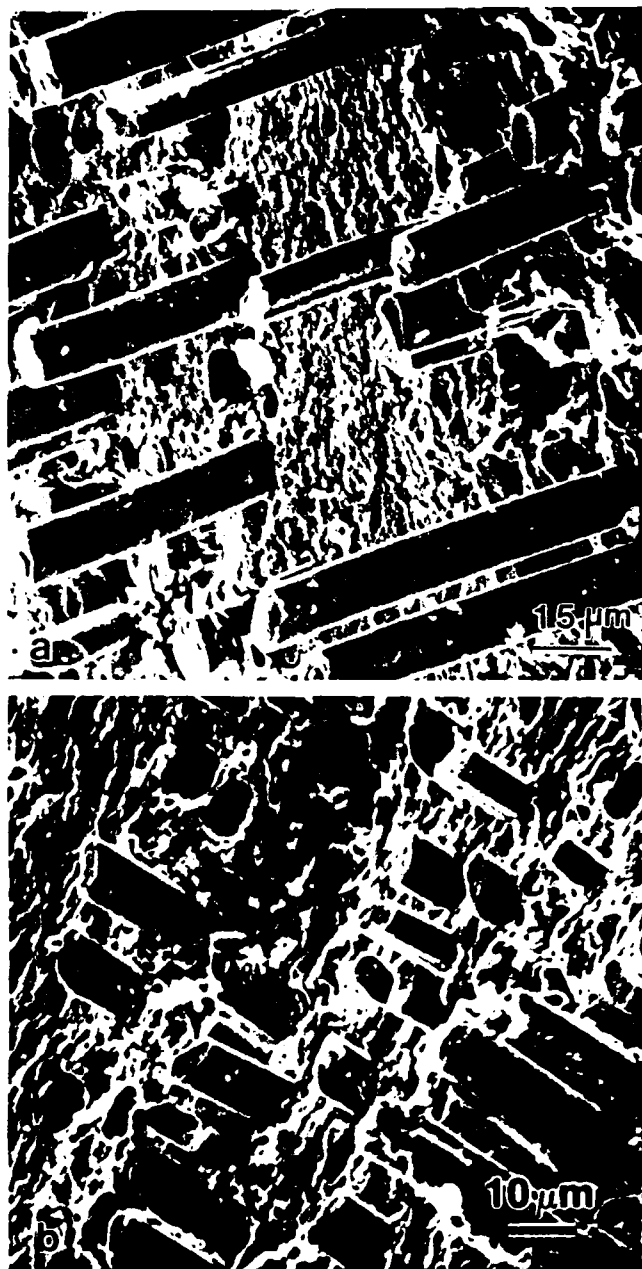


Figure 16